

UCSF

UC San Francisco Previously Published Works

Title

Design of a Short Thermally Stable α -Helix Embedded in a Macrocyclic

Permalink

<https://escholarship.org/uc/item/6tq0s79n>

Journal

ChemBioChem, 19(9)

ISSN

1439-4227

Authors

Wu, Haifan
Acharyya, Arusha
Wu, Yibing
et al.

Publication Date

2018-05-04

DOI

10.1002/cbic.201800026

Peer reviewed



Published in final edited form as:

Chembiochem. 2018 May 04; 19(9): 902–906. doi:10.1002/cbic.201800026.

Design of a Short Thermally Stable α -Helix Embedded in a Macrocycle

Haifan Wu^a, Arusha Acharyya^b, Yibing Wu^a, Lijun Liu^c, Hyunil Jo^a, Feng Gai^b, and William F. DeGrado^{*,a}

^[a]Department of Pharmaceutical Chemistry, University of California San Francisco, CA 94158 (USA)

^[b]Department of Chemistry, University of Pennsylvania Philadelphia, PA 19104 (USA)

^[c]DLX Scientific Lawrence, KS 66049 (USA)

Abstract

Although helices play key roles in peptide–protein and protein–protein interactions, the helical conformation is generally unstable for short peptides (10–15 residues) in aqueous solution in the absence of their binding partners. Thus, stabilizing the helical conformation of peptides can lead to increases in binding potency, specificity, and stability towards proteolytic degradation. Helices have been successfully stabilized by introducing side chain-to-side chain crosslinks within the central portion of the helix. However, this approach leaves the ends of the helix free, thus leading to fraying and exposure of the non-hydrogen-bonded amide groups to solvent. Here, we develop a “capped-strapped” peptide strategy to stabilize helices by embedding the entire length of the helix within a macrocycle, which also includes a semirigid organic template as well as end-capping interactions. We have designed a ten-residue capped-strapped helical peptide that behaves like a miniprotein, with a cooperative thermal unfolding transition and $T_m \approx 70^\circ\text{C}$, unprecedented for helical peptides of this length. The NMR structure determination confirmed the design, and X-ray crystallography revealed a novel quaternary structure with implications for foldamer design.

Keywords

capping interaction; constrained peptides; helical structures; mini-protein; peptide design

Nature makes extensive use of cyclic peptides in biology.^[1] The cyclic topology constrains the peptide conformation, thereby increasing stability and affinity for various targets.^[1,2] In particular, head-to-tail cyclization provides a high degree of stability because this restraint impacts the full structure and does not leave unrestrained loose ends.^[3] One prominent example of natural cyclic peptides is gramicidin S, in which short turns flank two β -strands to form a highly stabilized antiparallel β -hairpin.^[4]

*William F. DeGrado william.degrado@ucsf.edu.

Conflict of Interest

The authors declare no conflict of interest.

Supporting information and the ORCID identification numbers for the authors of this article can be found under <https://doi.org/10.1002/cbic.201800026>.

Stabilizing an α -helix within a small peptide is a difficult challenge that is sometimes fulfilled in natural peptides by the incorporation of α -methyl amino acids, which make a modest contribution towards helical stability.^[5] Alternatively, helices in small tertiary structures can be stabilized by disulfides and/or the formation of a peptide bond between the N- and C-terminal amino acids.^[6] A method to stabilize relatively long helices by buttressing them with a poly-proline II helix has also been reported.^[7] Nevertheless, these approaches result in relatively large peptides (>25 residues), so there has been considerable interest in the introduction of macrocycles within the interior positions of the α -helix to promote this conformation (“stapled peptides”, Figure 1A left).^[8] Another line of work has focused on the design of peptidic or nonpeptidic groups that stabilize helices through capping interactions (Figure 1A right).^[9] Although these approaches can increase helix stability, we sought to develop a method that would stabilize a full α -helix including its helical ends (Figure 1B).

Capping motifs are known to stabilize and rigidify α -helices and minimize the exposure of the terminal amides/carbonyls to water.^[10] When appropriately spaced at the ends of a helical peptide, N-cap and C-cap motifs provide convenient points for the attachment of a semirigid template to join the ends within a conformationally constraining macrocycle (capped-strapped). To provide a stringent test of the capped-strapped methodology, we sought to stabilize a relatively short 10-residue helix. Helix stability depends on chain length, and short monomeric helices are unstable in the absence of a tertiary structure or binding partners.^[11] Additionally, helices of this length comprise the binding hot-spots of many protein–protein interactions (PPIs).^[12] To design a capped-strapped helix, we first designed ideal capping sequences in favorable geometries, then built a semirigid linker to covalently bridge the capping motifs into a macrocycle (Figure 1B). At the N terminus, we chose a TPxQ motif for Nc–N3 (Figure 2A), following the nomenclature, N′-Nc-N1-N2-N3-N4...C1-Cc-C′-C′′, in which N1 and C1 denote the first and last helical residues, respectively.^[13] The N-terminal threonine forms a hydrogen-bonded Nc, proline at N1 serves as a helix-initiator,^[14] and glutamine at N3 further stabilizes N-cap through hydrogen-bonded interactions. At the C terminus, an ideal Schellman motif was employed, with a d-Ala residue at the C′ position followed by a Cys at C′′, to attach to the template.^[15] These interactions define the geometry of the helical ends, enabling the design of the linker for cyclization.

A bipartite linker that included both rigid elements to minimize conformational entropy as well as more flexible elements to assure sufficient flexibility to provide a strain-free fit between the linker and the peptide was chosen. Based on computational modeling, 4-thiobutyric acid (C*) was chosen as a partially flexible linker at the N′ position, and meta-substituted biphenyl linker (in capped-strapped peptide **1**, **CSP1**) and bipyridyl (in **CSP2**) were explored as elongated rigid templates. For comparison, we also synthesized N-capand C-cap-stabilized macrocyclic peptides (Figure 2A) according to a previously described strategy.^[16] In these peptides, key capping residues were retained as in **CSP1** and **CSP2**, but the macrocyclic link was formed to a side chain near the N or C terminus of the helix, rather than encompassing the entire helix. In each case, the peptides were cyclized by treating the

precursor with a bis-benzylic bromide to provide the bis-thioether macrocycle in good to excellent yields.

Far-UV circular dichroism (CD) spectroscopy and thermal unfolding indicate that **CSP1** and **CSP2** are almost fully helical between 08C and room temperature (Figure 2B, C). In contrast, the acyclic precursor is in a random-coil conformation, and the reference N-cap and C-cap peptides showed considerably lower helical contents. Furthermore, both capped-strapped peptides displayed high thermodynamic stability and a cooperative unfolding transition. Analysis of the equilibrium thermal melting (T-melt) gave T_m values of 69.7 and 52.7°C for **CSP1** and **CSP2**, respectively (Table 1), which are significantly greater than for the C-cap and N-cap peptides.

Importantly, both **CSP1** and **CSP2** lost their helical content in a cooperative transition, in a similar way to small proteins. The steepness (cooperativity) of a thermal-unfolding curve scales with the enthalpy of the transition, which is approximately -1 kcalmol⁻¹ per residue for helix formation.^[17] Interestingly, the enthalpy of folding of **CSP1**, -13.8 kcalmol⁻¹, exceeds that expected for a fully formed monomeric ten-residue α -helix, thus suggesting that the folded form is additionally stabilized by enthalpic interactions between the linker and the helix. The stability and cooperativity of **CSP2** is $1-2$ kcalmol⁻¹, less favorable than that of **CSP1**, thus indicating that the polarity and/or the inter-ring torsional angle of the bipyridyl is less conducive to helix stabilization than is the biphenyl group. Finally, the lower stability and cooperativity of the N-cap and C-cap peptides illustrates the contribution of the macrocyclic embedding of the entire helix in **CSP1** and **CSP2**.

We also measured the kinetics of folding and unfolding of **CSP2** by using laser-induced temperature-jump (T-jump) IR spectroscopy. **CSP2** was chosen for these experiments because **CSP1** partially associated at the low-millimolar concentrations required for the experiment (discussed in detail below). The IR relaxation kinetics in response to a laser-induced T-jump can be described by a single-exponential decay function (Figure S4C in the Supporting Information); this is consistent with two-state folding. This finding contrasts with the stretched exponentials previously seen for unrestrained capped peptides, which have more heterogeneous frayed helices.^[18] The relaxation rates were deconvoluted to reveal the folding and unfolding rates (Figure S4D).^[18] **CSP2** folds with a low enthalpic barrier of 7.4 kcalmol⁻¹, whereas unfolding occurs with an activation enthalpy of 21.8 kcalmol⁻¹; these are indicative of substantial breakage of hydrogen-bonded and van der Waals interactions in the high-energy state along the unfolding trajectory. At room temperature, the time constant for folding is 0.8 μ s, which is comparable to the rates seen for monomeric helices.^[19] Thus, the stability of **CSP2** derives from the slower unfolding rate (6.1 μ s) rather than an acceleration of folding.

To probe the contributions of specific interactions to the thermodynamic stability of **CSP1**, we synthesized a series of compounds with substitutions to the peptide and linker. Alanine substitutions of the Nc threonine and N3 glutamine decreased the helical content by approximately 40 and 30%, respectively, as assessed from the ellipticity at 222 nm, whereas substitutions at the N1 and N4 positions had little effect on helicity. The decrease in helicity associated with substitutions at Nc and N3 supports the importance of reciprocal hydrogen-

bonding between these residues; the relatively modest decrease in helicity associated with changes at these and other positions bodes well for the use of **CSP1** as a versatile platform for the presentation of a variety of sequences in a helical conformation. Similarly, substitution of the D-Ala (included to stabilize the α_{Left} conformation required for a Schellman capping motif), to glycine or alanine decreased helical content by 20 or 30%, respectively. Turning to linker substitutions, changing the 3,3'-substituted biphenyl with a 4,4' substitution pattern decreased the ellipticity by 40%. Replacing the 4-thiobutyric acid group with cysteine also decreased helicity by approximately 40%. In summary, these substitutions all confirm the principles employed in the design of **CSP1**, but even after these destabilizing mutations, the peptides retain a substantially greater ability to form helices than had been achieved in the N-cap and C-cap peptides. Thus, **CSP1** represents a robust scaffold for future studies in which substitutions might be required for function.

Concentration-dependent analytical ultracentrifugation and 1D NMR spectroscopy of **CSP1** (Figure S5) indicated that this miniprotein is fully monomeric at the low concentrations used in the above CD experiments (>90% monomeric at [**CSP1**] < 200 μM), but that it reversibly associates to form oligomers. The data were well described by either a monomer–hexamer or monomer–tetramer equilibrium, and, significantly, by other monomer–*n*-mer schemes involving either larger or small association states (Figure S9). Thus, it is likely that the hexamer is also weakly stable in aqueous solution. By contrast, **CSP2** with a more polar linker showed much less association over this concentration range (Figure S6). To probe the conformation of **CSP1** over a wide range of environments, we determined structures of the monomer by solution NMR spectroscopy (at 156 μM) and of the hexamer by X-ray crystallography.

The solution NMR structure of **CSP1** (Figure 3A) is fully consistent with its design. The structure was well-defined by 26 medium-range, 22 long-range, and 22 peptide-crosslinker NOEs, as well as 20 torsion-angle restraints from Talos.^[20] The ensemble of the 20 lowest-energy conformers (computed by using XPLOR-NIH^[21]) is well defined, with a backbone heavy-atom root-mean-square deviation (RMSD) of (0.39 ± 0.12) Å. The overall structure conforms extremely well with the design, including the presence of helix-capping motifs (discussed in more detail below). Hydrogen/deuterium exchange (HDX) in **CSP1** provided further evidence of the overall stability of the helical secondary structure, including the capping motifs. In the designed and the experimentally determined structure of **CSP1**, the backbone amide of Arg4 is the only backbone amide NH that is not engaged in helical or capping hydrogen-bond interactions, and hence was expected to exchange rapidly with solvent deuterons, when dissolved in D₂O. Indeed, the Arg4 backbone amide showed complete exchange within the dead-time (12 min) of detection by NMR spectroscopy (Figure 3B), whereas the amide protons of the remaining residues were protected from hydrogen/deuterium exchange as a result of hydrogen bonding (Table S3). Interestingly, residues at the helical ends showed even larger degrees of protection; thus suggesting that the capping motifs might be retained in the small fraction of the peptide that is in the unfolded ensemble at any given time. Thr2, at Nc, displayed slowest exchange; this is likely due to the shielding by the Thr2 γ -methyl group and strong hydrogen bonding with the Gln5 side chain.

The 1.25 Å-resolution crystal structure of **CSP1** (Figure 4A) revealed a novel hexameric assembly, in which the peptidic portions of **CSP1** conform precisely to the design. The helix and N- and C-cap interactions are as in the designed model, including the predicted side chain-to-backbone hydrogen bonds (Figure 4C, red dashes). Moreover, the backbone dihedral angles (Table S2) of Thr2 (Nc), Ala12 (Cc) and d-Ala13 (C') closely resemble those in the N-capping box and Schellman motifs. The overall quaternary structure of the hexamer is also of considerable interest. The oligomer is stabilized by a hydrophobic core that is composed entirely of well-packed biphenyl linkers. Thus, our structure provides a striking example of a foldamer-like structure with an entirely artificial hydrophobic core unlike anything seen in natural proteins. The packing of the biphenyl linkers positions individual helices in an antiparallel orientation, with small-into-small packing of alanine residues on opposing interfaces. The packing between the individual helices could be optimized in future studies. Thus, this serendipitous discovery expands the repertoire of building blocks available to chemists for the design of foldamers^[22] and protein mimics unprecedented in nature.

In addition to the implications for the de novo design of foldamers with well-defined tertiary structures, the structure of **CSP1** has significant implications for the design of stabilized helices as inhibitors of protein–protein and protein–peptide interactions. The retention of helical structure between the monomeric solution structure and the hexameric crystal structure speaks of the robustness of the scaffold over a range of environments.

Superposition of the individual monomers in the crystal structure with those computed for the solution ensemble shows that the linker is able to adjust its conformation to enable interchain packing without perturbing the helical conformation (Figure 4B). This limited flexibility might ultimately prove useful for molecular recognition, in which both the peptide and the biphenyl could be varied to optimize the affinity of a given interaction. Indeed, the linkers of stapled peptides have already been shown to contribute to binding to protein targets.^[12c] Hydrophobic moieties are known to cause poor solubility, aggregation, and nonspecific interactions,^[23] and this should be borne in mind when designing protein binders. However, we have shown that the more polar bipyridyl linker is well tolerated. Thus, the substitution of biphenyl with bipyridyl in capped-strapped peptides should be a solution to the potential problem.

In conclusion, we have presented a helix-stabilizing strategy through incorporating a short α -helix into a macrocycle template. The ten-residue helix is rigid even at its ends and showed high thermodynamic stability. This ideal helical scaffold folds cooperatively as a mini-protein and provides opportunities for the design of novel tertiary and quaternary architectures and inhibitors of protein–protein interactions.

Supplementary Material

Refer to Web version on PubMed Central for supplementary material.

Acknowledgements

W.F.D. and F.G. are supported by grants from the National Institutes of Health (GM122603 and GM104605, respectively). Beamline 8.3.1 at the Advanced Light Source is operated by the University of California Office of the

President, Multicampus Research Programs and Initiatives grant MR-15-328599, the National Institutes of Health (R01 GM124149 and P30 GM124169), Plexxikon Inc. and the Integrated Diffraction Analysis Technologies program of the US Department of Energy Office of Biological and Environmental Research. The Advanced Light Source (Berkeley, CA) is a national user facility operated by Lawrence Berkeley National Laboratory on behalf of the US Department of Energy under contract number DE-AC02-05CH11231, Office of Basic Energy Sciences. We thank Dr. Shao-Qing Zhang for the help with AUC experiments.

References

- [1]. Bockus AT, McEwen CM, Lokey RS, *Curr. Top. Med. Chem* 2013, 13, 821–836. [PubMed: 23578026]
- [2]. a) Clark RJ, Jensen J, Nevin ST, Callaghan BP, Adams DJ, Craik DJ, *Angew. Chem. Int. Ed* 2010, 49, 6545–6548; *Angew. Chem.* 2010, 122, 6695–6698; b) Clark RJ, Fischer H, Dempster L, Daly NL, Rosengren KJ, Nevin ST, Meunier FA, Adams DJ, Craik DJ, *Proc. Natl. Acad. Sci. USA* 2005, 102, 13767–13772. [PubMed: 16162671]
- [3]. a) Craik DJ, *Science* 2006, 311, 1563–1564; [PubMed: 16543448] b) Trabi M, Craik DJ, *Trends Biochem. Sci* 2002, 27, 132–138. [PubMed: 11893510]
- [4]. a) Kondejewski LH, Farmer SW, Wishart DS, Kay CM, Hancock RE, Hodges RS, *J. Biol. Chem* 1996, 271, 25261–25268; [PubMed: 8810288] b) Yamada K, Unno M, Kobayashi K, Oku H, Yamamura H, Araki S, Matsumoto H, Katakai R, Kawai M, *J. Am. Chem. Soc* 2002, 124, 12684–12688. [PubMed: 12392415]
- [5]. O'Neil KT, DeGrado WF, *Science* 1990, 250, 646–651. [PubMed: 2237415]
- [6]. a) Bhardwaj G, Mulligan VK, Bahl CD, Gilmore JM, Harvey PJ, Cheneval O, Buchko GW, Pulavarti SV, Kaas Q, Eletsky A, Huang PS, Johnsen WA, Greisen PJ, Rocklin GJ, Song Y, Linsky TW, Watkins A, Rettie SA, Xu X, Carter LP, Bonneau R, Olson JM, Coutsiadis E, Correnti CE, Szyperski T, Craik DJ, Baker D, *Nature* 2016, 538, 329–335; [PubMed: 27626386] b) Dang B, Wu H, Mulligan VK, Mravic M, Wu Y, Lemmin T, Ford A, Silva DA, Baker D, DeGrado WF, *Proc. Natl. Acad. Sci. USA* 2017, 114, 10852–10857. [PubMed: 28973862]
- [7]. a) Baker EG, Williams C, Hudson KL, Bartlett GJ, Heal JW, Porter Goff KL, Sessions RB, Crump MP, Woolfson DN, *Nat. Chem. Biol* 2017, 13, 764–770; [PubMed: 28530710] b) Zondlo NJ, Schepartz A, *J. Am. Chem. Soc* 1999, 121, 6938–6939; c) Chin JW, Schepartz A, *J. Am. Chem. Soc* 2001, 123, 2929–2930. [PubMed: 11456999]
- [8]. a) Felix AM, Heimer EP, Wang CT, Lambros TJ, Fournier A, Mowles TF, Maines S, Campbell RM, Wegrzynski BB, Toome V, et al., *Int. J. Pept. Protein Res* 1988, 32, 441–454; [PubMed: 3149952] b) Blackwell HE, Grubbs RH, *Angew. Chem. Int. Ed* 1998, 37, 3281–3284; *Angew. Chem.* 1998, 110, 3469–3472; c) Schafmeister CE, Po J, Verdine GL, *J. Am. Chem. Soc* 2000, 122, 5891–5892; d) Pelay-Gimeno M, Glas A, Koch O, Grossmann TN, *Angew. Chem. Int. Ed* 2015, 54, 8896–8927; *Angew. Chem.* 2015, 127, 9022–9054; e) Jackson DY, King DS, Chmielewski J, Singh S, Schultz PG, *J. Am. Chem. Soc* 1991, 113, 9391–9392; f) Shepherd NE, Hoang HN, Abbenante G, Fairlie DP, *J. Am. Chem. Soc* 2005, 127, 2974–2983; [PubMed: 15740134] g) Zhang F, Sadowski O, Xin SJ, Woolley GA, *J. Am. Chem. Soc* 2007, 129, 14154–14155; [PubMed: 17960932] h) Lau YH, de Andrade P, Wu Y, Spring DR, *Chem. Soc. Rev* 2015, 44, 91–102; [PubMed: 25199043] i) Timmerman P, Beld J, Puijk WC, Meloen RH, *ChemBioChem* 2005, 6, 821–824; [PubMed: 15812852] j) Spokoynny AM, Zou Y, Ling JJ, Yu H, Lin YS, Pentelute BL, *J. Am. Chem. Soc* 2013, 135, 5946–5949; [PubMed: 23560559] k) Diderich P, Bertoldo D, Dessen P, Khan MM, Pizzitola I, Held W, Huelsken J, Heinis C, *ACS Chem. Biol* 2016, 11, 1422–1427; [PubMed: 26929989] l) Yu H, Dranchak P, Li Z, MacArthur R, Munson MS, Mehzabeen N, Baird NJ, Battalio KP, Ross D, Lovell S, Carlow CK, Suga H, Inglese J, *Nat. Commun* 2017, 8, 14932; [PubMed: 28368002] m) Kodan A, Yamaguchi T, Nakatsu T, Sakiyama K, Hipolito CJ, Fujioka A, Hirokane R, Ikeguchi K, Watanabe B, Hiratake J, Kimura Y, Suga H, Ueda K, Kato H, *Proc. Natl. Acad. Sci. USA* 2014, 111, 4049–4054; [PubMed: 24591620] n) Harrison RS, Shepherd NE, Hoang HN, Ruiz-Gomez G, Hill TA, Driver RW, Desai VS, Young PR, Abbenante G, Fairlie DP, *Proc. Natl. Acad. Sci. USA* 2010, 107, 11686–11691. [PubMed: 20543141]
- [9]. a) Schneider JP, DeGrado WF, *J. Am. Chem. Soc* 1998, 120, 2764–2767; b) Maison W, Arce E, Renold P, Kennedy RJ, Kemp DS, *J. Am. Chem. Soc* 2001, 123, 10245–10254; [PubMed:

- 11603974] c) Patgiri A, Jochim AL, Arora PS, *Acc. Chem. Res* 2008, 41, 1289–1300; [PubMed: 18630933] d) Johnson LM, Gellman SH, *Methods Enzymol.* 2013, 523, 407–429; [PubMed: 23422441] e) Fremaux J, Mauran L, Pulka-Ziach K, Kauffmann B, Odaert B, Guichard G, *Angew. Chem. Int. Ed* 2015, 54, 9816–9820; *Angew. Chem.* 2015, 127, 9954–9958; f) Tian Y, Wang D, Li J, Shi C, Zhao H, Niu X, Li Z, *Chem. Commun* 2016, 52, 9275–9278; g) Hoang HN, Driver RW, Beyer RL, Hill TA, de Araujo AD, Plisson F, Harrison RS, Goedecke L, Shepherd NE, Fairlie DP, *Angew. Chem. Int. Ed* 2016, 55, 8275–8279; *Angew. Chem.* 2016, 128, 8415–8419; h) Cabezas E, Satterthwait AC, *J. Am. Chem. Soc* 1999, 121, 3862–3875; i) Nguyen LT, Luong HX, Kim YW, *Bull. Korean Chem. Soc* 2016, 37, 566–570; j) Hoang HN, Wu CY, Beyer RL, Hill TA, Fairlie DP, *Aust. J. Chem* 2017, 70, 213–219.
- [10]. Aurora R, Rose GD, *Protein Sci.* 1998, 7, 21–38. [PubMed: 9514257]
- [11]. Qian H, Schellman JA, *J. Phys. Chem* 1992, 96, 3987–3994.
- [12]. a) Bernal F, Wade M, Godes M, Davis TN, Whitehead DG, Kung AL, Wahl GM, Walensky LD, *Cancer Cell* 2010, 18, 411–422; [PubMed: 21075307] b) Phillips C, Roberts LR, Schade M, Bazin R, Bent A, Davies NL, Moore R, Pannifer AD, Pickford AR, Prior SH, Read CM, Scott A, Brown DG, Xu B, Irving SL, *J. Am. Chem. Soc* 2011, 133, 9696–9699; [PubMed: 21612236] c) Stewart ML, Fire E, Keating AE, Walensky LD, *Nat. Chem. Biol* 2010, 6, 595–601. [PubMed: 20562877]
- [13]. Richardson JS, Richardson DC, *Science* 1988, 240, 1648–1652. [PubMed: 3381086]
- [14]. Yun RH, Anderson A, Hermans J, *Proteins* 1991, 10, 219–228. [PubMed: 1881878]
- [15]. Schellman C, Hoppe-Seyler's *Z Physiol. Chem* 1979, 360, 1014–1015.
- [16]. a) Jo H, Meinhardt N, Wu Y, Kulkarni S, Hu X, Low KE, Davies PL, DeGrado WF, Greenbaum DC, *J. Am. Chem. Soc* 2012, 134, 17704–17713; [PubMed: 22998171] b) Findeisen F, Campiglio M, Jo H, Abderemane-Ali F, Rumpf CH, Pope L, Rossen ND, Flucher BE, DeGrado WF, Minor DL Jr., *ACS Chem. Neurosci* 2017, 8, 1313–1326. [PubMed: 28278376]
- [17]. Scholtz JM, Marqusee S, Baldwin RL, York EJ, Stewart JM, Santoro M, Bolen DW, *Proc. Natl. Acad. Sci. USA* 1991, 88, 2854–2858. [PubMed: 2011594]
- [18]. Wang T, Zhu Y, Getahun Z, Du D, Huang C-Y, DeGrado WF, Gai F, *J. Phys. Chem. B* 2004, 108, 15301–15310.
- [19]. Huang CY, Klemke JW, Getahun Z, DeGrado WF, Gai F, *J. Am. Chem. Soc* 2001, 123, 9235–9238. [PubMed: 11562202]
- [20]. Shen Y, Delaglio F, Cornilescu G, Bax A, *Biomol J NMR* 2009, 44, 213–223.
- [21]. a) Schwieters CD, Kuszewski JJ, Tjandra N, Clore GM, *J. Magn. Reson* 2003, 160, 65–73; [PubMed: 12565051] b) Schwieters CD, Kuszewski JJ, Clore GM, *Prog. Nucl. Magn. Reson. Spectrosc* 2006, 48, 47–62.
- [22]. a) Gellman SH, *Acc. Chem. Res* 1998, 31, 173–180; b) Hill DJ, Mio MJ, Prince RB, Hughes TS, Moore JS, *Chem. Rev* 2001, 101, 3893–4012. [PubMed: 11740924]
- [23]. Gaillard V, Galloux M, Garcin D, Eleouet J-F, Le Goffic R, Larcher T, Rameix-Welti M-A, Boukadiri A, Heritier J, Segura J-M, Baechler E, Arrell M, Mottet-Osman G, Nyanguile O, *Antimicrob. Agents Chemother.* 2017, 61, e02241–16. [PubMed: 28137809]

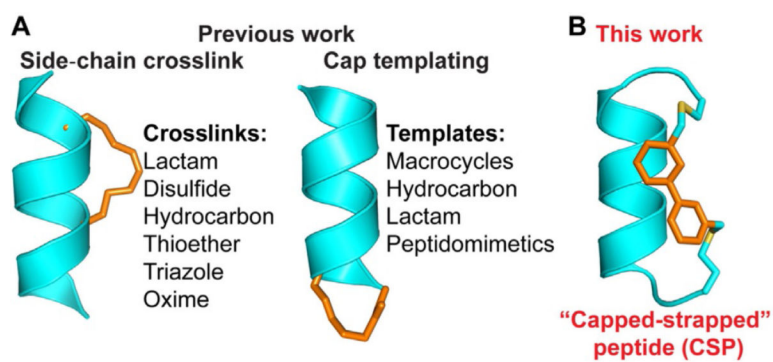


Figure 1.

A) Previous reported strategies for stabilizing short, helical peptides. B) The capped-strapped method in this study.

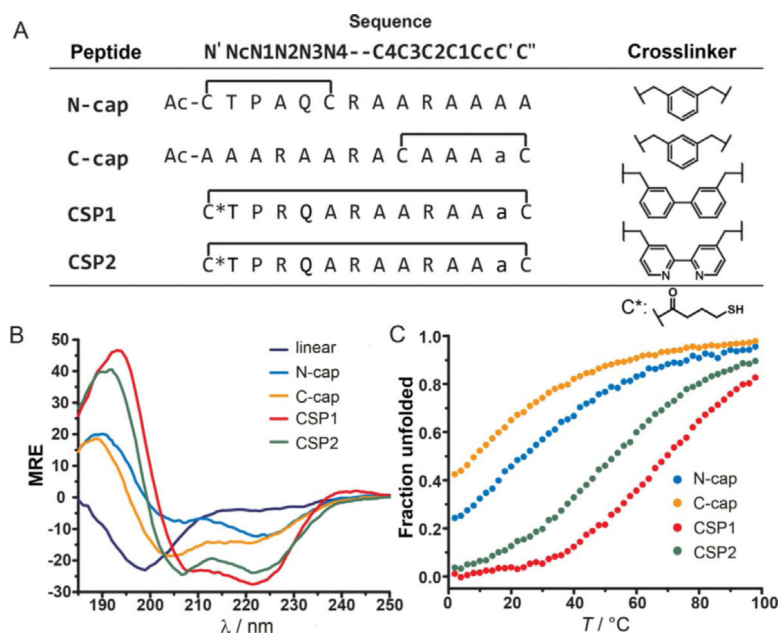


Figure 2. Helical structures of peptides probed by CD spectroscopy. A) Sequences of singly capped peptides and capped-strapped peptides. B) CD spectra obtained at 25°C expressed as mean residue ellipticity [$10^3 \text{ deg cm}^2 \text{ dmol}^{-1} \text{ res}^{-1}$]. C) Thermal unfolding of the peptides. All CD measurements were conducted at 50 μm in 10 mM phosphate buffer (pH 7.4).

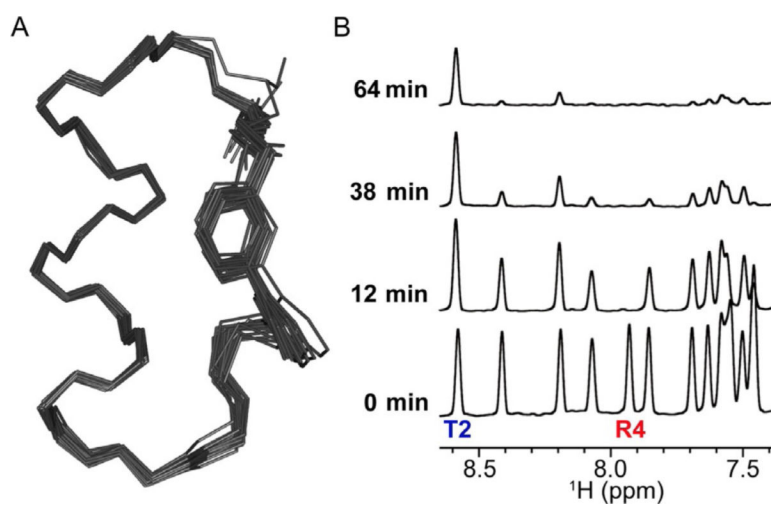


Figure 3. Structural studies of **CSP1** by solution NMR spectroscopy (PDB ID: 6ANF). A) The ensemble of 20 lowest-energy NMR structures. Side chains and carbonyls are omitted for clarity. Backbone heavy-atom RMSD: (0.39 ± 0.12) Å. B) Probing the backbone hydrogen bonding by hydrogen/deuterium exchange (HDX). NMR studies were conducted at 156 μm in 100 mm acetate buffer (pH 4.1).

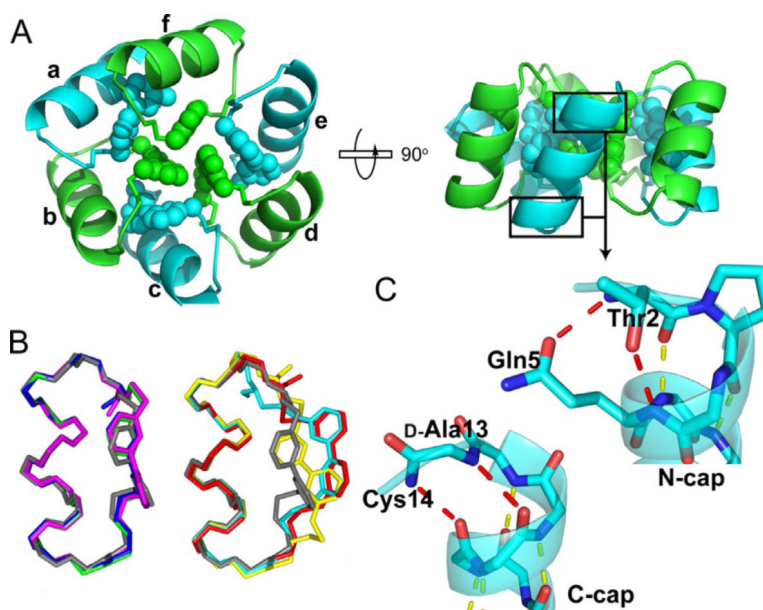


Figure 4. CSP1 is shown to form a hexamer by X-ray crystallography (PDB ID: 6B17). A) Hexameric packing in the crystal structure. B) Superposition of chains a (green)/c (magenta)/e (blue) and b (red)/d (cyan)/f (yellow) in the crystal structure with the lowest-energy (grey) NMR structure. C) Hydrogen bonding stabilizes the structure. Yellow: intrahelical hydrogen bonds; red: hydrogen bonds involving capping residues.

Table 1.

Thermodynamic parameters for the folding of peptides derived from thermal melting curves. The parameters were obtained by nonlinear least-squares fitting of the Gibbs–Helmholtz equation and assuming the change in heat capacity (ΔC_p) to be zero.

Peptide	T_m [°C]	H_{fold} [kcalmol ⁻¹]	S_{fold} [kcalmol ⁻¹ K ⁻¹]	$G_{\text{fold}}^{[a]}$ [kcalmol ⁻¹]	$\theta_{222}^{[b]}$ [degcm ² dmol ⁻¹ res ⁻¹]
N-cap	24.1±1.3	-8.7±0.6	-0.029	-0.7	-17700
C-cap	8.3±1.9	-8.3±0.5	-0.029	-0.2	-23400
CSP1	69.7±0.6	-13.8±0.5	-0.040	-2.8	-28800
CSP2	52.7±0.8	-11.6±0.3	-0.035	-1.9	-27200

^[a] at 0°C.

^[b] at 2°C.